3. Moertel CG. An odyssey in the land of small tumors. *J Clin Oncol* 1987;5:1503–1522.
4. Vinik AI, McLeod MK, Fig LM, et al. Clinical features, diagnosis and localization of carcinoid tumors and their management. *Gastroenterol Clin North Am* 1989;18:865–896.
5. Kvols LK, Moertel CG, O'Connel MJ, Schutt AJ, Rubin J, Hahn RG. Treatment of the malignant carcinoid syndrome: evaluation of a long-acting somatostatin analogue. *N Engl J Med* 1986;315:663–666.
6. Kvols LK, Reubi JC. Metastatic carcinoid tumors and the malignant carcinoid syndrome. *Acta Oncol* 1993;32:197–201.
7. Feldman JM, Blinder RA, Lucas KJ, Coleman RE. Iodine-131 metaiodobenzylguanidine scintigraphy of carcinoid tumors. *J Nucl Med* 1986;27:1691–1696.
8. Hanson MW, Feldman JM, Blinder RA, Moore JO, Coleman RE. Carcinoids tumors: iodine-131 MIBG scintigraphy. *Radiology* 1989;172:699–703.
9. Lamberts SWJ, Bakker WH, Reubi JC, et al. Somatostatin receptors imaging in the localization of endocrine tumors. *N Engl J Med* 1990;323:1246–1249.
10. Kvols LK, Brown ML, O'Connor MK, et al. Evaluation of a radiolabeled somatostatin analog (^{123}I-octreotide) in the detection and localization of carcinoid and islet cells tumors. *Radiology* 1993;49:1583–1591.
11. Bakker WH, Albert R, Bruns C, et al. Indium-111-DTPA-D-Phe^1-octreotide, a potential radiopharmaceutical for imaging of somatostatin receptor-positive tumors: synthesis, radiolabeling and in vitro validation. *Life Sci* 1991;49:1583–1591.
12. Bakker WH, Krenning EP, Reubi JC, et al. In vivo application of [^{111}In-DTPA-D-Phe^1]-octreotide for detection of somatostatin receptor-positive tumors in rats. *Life Sci* 1991;49:1593–1601.
13. Kwekkeboom DS, Krenning EP, Bakker WH, Oei HJ, Kooij PPM, Lamberts SWJ. Somatostatin analogue scintigraphy in carcinoid tumors. *Eur J Nucl Med* 1993;20:283–292.
14. Carnaille B, Nocadudie M, Pattou F, et al. Scintiscans and carcinoid tumors. *Surgery* 1994;116:1118–1122.
15. Simpson S, Vinik AI, Harangos PJ, Lloyd RV. Immunohistochemical localization of neuron-specific enolase in gastroenteropancreatic neuroendocrine tumors. Correlation with tissue and serum level of neuron-specific enolase. *Cancer* 1984;54:1364–1369.
16. Nash SU, Said JW. Gastroenteropancreatic neuroendocrine tumors: a histochemical and immunohistochemical study of epithelial (keratin proteins, carcinoembryonic antigen) and neuroendocrine (neuron-specific enolase, bombesin and chomogranin) markers in foregut, midgut, and hindgut tumors. *Am J Clin Pathol* 1986;86:415–422.
17. Zimmer T, Ziegler K, Bader M, et al. Localization of neuroendocrine tumors of the upper gastrointestinal tract. *Gut* 1994;35:471–475.
18. Picus D, Glazer HS, Levitt RG, Husband JE. Computed tomography of abdominal carcinoid tumors. *AJR* 1984;143:581–584.
19. McCarthy SM, Stark DD, Moss AA, Goldberg HI. Computed tomography of malignant carcinoid disease. *J Comput Assist Tomogr* 1984;8:846–850.
20. Kressel HY. Strategies for magnetic resonance imaging of focal liver disease. *Radiol Clin North Am* 1988;26:607–617.
21. Li K, Glazer GM, Quint LE, et al. Distinction of hepatic cavernous hemangioma from hepatic metastases with MR imaging. *Radiology*, 1988;169:409–415.
22. Bomanji J, Levison DA, Zuzarte J, Britton KE. Imaging of carcinoid tumors with ^{123}I-metaiodobenzylguanidine. *J Nucl Med* 1987;28:1907–1910.
23. Hoefnagel CA, den Hartog Jager FCA, Taal BG, Abeling NGGM, Engelsman EE. The role of ^{131}I-MIBG in the diagnosis and therapy of carcinoids. *Eur J Nucl Med* 1987;13:187–191.
24. Hoefnagel CA. Metaiodobenzyl-guanidine and somatostatin in oncology: role in the management of neural crest tumors. *Eur J Nucl Med* 1994;21:561–581.
25. Lamberts SWJ, Krenning EP, Reubi JC. The role of somatostatin and its analogs in the diagnosis and treatment of tumors. *Endocrinol Rev* 1991;21:450–482.
26. Bonanji J, Ur E, Mather S, et al. A scintigraphic comparison of iodine-123-metaiodobenzylguanidine and an iodine-labeled somatostatin analogue (tyr-3-octreotide) in metastatic carcinoids tumors. *J Nucl Med* 1992;33:1121–1124.
27. Krenning EP, Bakker WH, Kooij PPM, et al. Somatostatin receptor scintigraphy with indium-111-DTPA-D-phe1-octreotide in man: metabolism, dosimetry and comparison with iodine-123-tyr-3-octreotide. *J Nucl Med* 1992;33:652–658.
28. Schillaci O, Scopinaro F, Di Macio L, et al. Detection of malignant endocrine tumors with ^{111}In-octreoscan and SPECT [abstract]. *J Nucl Biol Med* 1994;38:341–342.
29. Pauwels S, Leners S, Fiasse R, Jamar F. Localization of gastroenteropancreatic neuroendocrine tumors with ^{111}indium-pentetreotide scintigraphy. *Semin Oncol* 1994; 21(suppl 13):15–20.
30. Jamar F, Fiasse R, Leners N, Pauwels S. Somatostatin receptor imaging with indium-111-pentetreotide in gastroenteropancreatic neuroendocrine tumors: safety, efficacy and impact on patient management. *J Nucl Med* 1995;36:542–549.
31. Krenning EP, Kwekkeboom DJ, Bakker WH, et al. Somatostatin receptor scintigraphy with [^{111}in-DTPA-D-Phe^1]- and [^{123}I-tyr^3]-octreotide: the Rotterdam experience with more than 1000 patients. *Eur J Nucl Med* 1993;20:716–731.
32. Pellizzari CA, Chen GTY, Spelbring DR, Weichselbaum RR, Chen CT. Accurate three-dimensional registration of CT, PET, and/or MR images of the brain. *J Comput Assist Tomogr* 1989;13:20–26.
33. Kessler ML, Pitluck S, Petti P, Castro JR. Integration of multimodality imaging data for radiotherapy treatment planning. *Int J Radiat Oncol Biol Phys* 1991;21:1653–1667.
34. Scott AM, Macapinlac HA, Divgi CR, et al. Clinical validation of SPECT and CT/MRI image registration in radiolabeled monoclonal antibody studies of colorectal carcinoma. *J Nucl Med* 1994;35:1976–1984.
35. Scott AM, Macapinlac H, Zhang JJ, et al. Clinical applications of fusion imaging in oncology. *Nucl Med Biol* 1994;21:775–784.

Bone Scintigraphy Evaluated in Diagnosing and Staging Langerhans' Cell Histiocytosis and Related Disorders

Douglas M. Howarth, Brian P. Mullan, Gregory A. Wiseman, Doris E. Wenger, Lee A. Forstrom and William L. Dunn
Department of Nuclear Medicine and Diagnostic Radiology, Mayo Clinic, Rochester, Minnesota

An analysis of patients with proven Langerhans' cell histiocytosis (LCH) was undertaken with the aim of evaluating the role of bone scintigraphy in the diagnosis and staging of LCH. **Methods:** Radiographic skeletal surveys and whole-body bone scintigraphy study results were reviewed for all patients treated at the Mayo Clinic in Rochester, Minnesota during 1965–1994 with histologic proven LCH. All available studies were then reported in a randomized and blinded fashion. **Results:** Of the 73 patients with the histologic diagnosis, 56 (76%) had a definite lesion reported on radiographs and subsequent biopsy-proven bone involvement. For this population, the sensitivity and specificity of radiographic survey were 100% and 61%, respectively, compared to 91% and 55% for bone scintigraphy. Solitary bone lesions were reported on 21 radiographic surveys and 24 bone scintigrams. For solitary lesions, radiograph sensitivity and specificity were 95% and 73%, respectively, compared to 88% and 77% for bone scintigraphy. Bone scintigraphy receiver operating characteristic curves showed the region of greatest diagnostic accuracy to be skull, facial bones and mandible (88% sensitivity, 52% specificity). Radiation dosimetry to adult reproductive organs was less favorable for radiographic skeletal survey compared to bone scintigraphy. **Conclusion:** Our results support the use of radiographic skeletal survey in the initial diagnosis of LCH. Bone scintigraphy may have a role in monitoring a patient's progress in which the initial scintigram and radiographic survey show good correlation.

Key Words: bone scintigraphy; Langerhans' cell histiocytosis

J Nucl Med 1996; 37:1456–1460

The diverse group of diseases associated with Langerhans' cell proliferation encompass a disparate group of clinical presentations, clinical courses and responses to treatment. They all display, however, abnormal proliferation of histiocytes, the cell class to which the Langerhans' cell belongs. Only recently has the classification and nomenclature of these diseases been standardized. The recommended term, Langerhans' cell histiocytosis (LCH) represents diseases that were previously known as eosinophilic granuloma, histiocytosis X, Langerhans' cell granulomatosis and classified into unifocal or multifocal subtypes (*1*). Syndromes such as Hand-Schuller-Christian disease

Received May 22, 1995; revision accepted Dec. 13, 1995.
For correspondence or reprints contact: Douglas M. Howarth, MD, Department of Nuclear Medicine, John Hunter Hospital Locked Bag No. 1, Newcastle Mail Centre, Newcastle, 2310 NSW, Australia.

and the Letterer-Siwe disease are included in this spectrum, but each disease also exhibits their own unique clinical characteristics.

Skeletal radiology is generally regarded as the most accurate means of detecting bone lesions due to LCH (*2*). Bone scintigraphy has also been advocated as having a role in the diagnosis and staging of LCH but as yet has not been thoroughly evaluated (*3*). The objective of this study was to evaluate the role of bone scintigraphy in the diagnosis and staging of LCH and related disorders.

MATERIALS AND METHODS

After Institutional Review Board approval, a retrospective analysis of patient records at the Mayo Clinic in Rochester Minnesota was undertaken for the period 1965–1994. Accurate and consistent record keeping permitted reliable data extraction from the records of those patients who had a biopsy-proven diagnosis of LCH, whole-body bone scintigraphy and radiographic skeletal survey. For each of these patients, all available skeletal survey radiograph films and bone scintigrams were reviewed and reported in randomized and blinded fashion by a radiologist and nuclear medicine physicians, respectively. All reports were structured into skeletal regional analysis, allowing qualitative and semiquantitative description of each study. The anatomic regions were graded as: 1 = normal; 2 = abnormal probably benign; 3 = abnormal possibly LCH; and 4 = abnormal definitely LCH. Radiographic skeletal surveys were reported by a radiologist who was aware only that each patient was being evaluated for the presence or absence of LCH and was given no other clinical details. Bone scintigrams were independently reported by two nuclear medicine physicians, one with (NP 1) and one without (NP 2) information, including each patient's clinical history, physical examination findings and radiograph findings. Intraobserver reproducibility was tested by a third nuclear medicine physician (NP 3) who independently reported each patient's study initially and then again after 6 wk.

Sensitivity, specificity, positive predictive value and accuracy were determined by 4 × 4 tables using the bone biopsy result as the criterion for disease presence or absence. For these calculations of the reported bone scans, true disease status was determined on the basis of the radiographic results of biopsy-proven LCH patients in whom Grades 1 and 2 were considered as disease absent and Grades 3 and 4 as disease present. Bone scintigraphy reports by NP 1 and NP 2 were compared on a regional basis using area (A1 and A2) and standard error (SE1 and SE2) under the receiver operating characteristic curves calculated using the Dorfman and Alf maximum likelihood estimation program. The correlation coefficients for ratings given to images from diseased (r_A) and nondiseased (r_N) regions were calculated by the Kendall tau correlation and the mean (r) determined. Probability (p) was then derived from the Z score using the equation:

$$Z = (A1 - A2)(SE1^2 + SE2^2 - 2rSE1SE2)^{-1/2}\ (4,5).$$

Planar bone scintigraphy was performed approximately 4 hr after intravenous injection of ^{99m}Tc-methylene diphosphonate (adult dose 740 MBq, pediatric dose 16.8 MBq/kg). Technetium-99m-pyrophosphate was used for the 21 studies performed before 1978. Imaging was to 1000K counts per local view and/or 15 cm/min for whole-body sweeps using a high-resolution, parallel-hole collimator. The skeletal bone survey included: radiographs of the skull, facial bones, axial skeleton and appendicular skeleton where clinically indicated.

Diagnosis was made on the basis of the histopathology biopsy specimen showing multinucleated Langerhans' cells, histiocytes and eosinophils. The presence of Birbeck granules on electron microscopic examination or the antigenic surface markers that react with OK6/Leu6 antibody and the cytoplasmic protein S 100 detected by immunoperoxidase staining methods were sought in cases where further confirmatory diagnostic evidence was required. The patient follow-up period ranged from 1 mo to 24 yr and 4 mo (mean = 7 yr–3 mo). Prolonged remission was defined as no new lesions after 5 yr and radiologic improvement of bone lesions.

Radiation dosimetry for whole-body radiograph skeletal survey and bone scintigraphy was calculated for both a 70 kg adult and a 15 kg child. Radiographic dosimetry was calculated by determining x-ray output in mGy per mAs at 1 meter for 2.5 mm aluminium total filtration (×1.8 three-phase correction) and the kVp for the particular radiograph technique. A 5-cm distance between skin surface and film and inverse square calculation were used to determine x-ray tube output at the patient. Average absorbed doses were then determined from ICRP 34 tables (*6*). Bone scintigraphy dosimetry was based on previously published data for both adults and children (*7,8*).

RESULTS

The histologic diagnosis of LCH was made in 73 patients who had radiograph surveys and bone scintigraphy between March 1965 and November 1994. Age at the time of diagnosis ranged between 6 mo and 83 yr (mean age 28 ± 18 yr). The male-to-female ratio was 41:32. Of these patients, 56 (76%) had a definite lesion reported on radiographs and subsequent biopsy-proven bone involvement (Table 1). Bone scintigraphy showed abnormal radiotracer uptake in the region of suspected involvement in 51 patients. The sensitivity and specificity of radiographic survey for the detection of LCH in this patient population were 100% and 61%, respectively, compared to 91% and 55% for bone scintigraphy. Overall, for detection of disease in the 73 patients, the accuracy of skeletal radiograph survey was 90% compared to 82% for bone scintigraphy.

Typical radiographic appearance of LCH was that of a lucent lesion, sometimes well circumscribed, often with sclerotic margins and a bevelled edge. Analysis of lesions seen on 28 skeletal radiograph surveys showed 45% to be lucencies, 9% sclerotic lesions, 42% mixed lucent and sclerotic lesions and 4% complicated lesions e.g., involving vertebral compression fracture. LCH on bone scintigraphy typically appeared as a focus of avid tracer uptake or, alternatively, a circumscribed rim of increased radiotracer activity surrounding a photopenic region (Figs. 1, 2). After local radiotherapy or systemic chemotherapy, radiotracer distribution more diffuse and often less avid (Fig. 3).

Solitary bone lesions were reported on 21 radiograph surveys and 29 bone scans. These lesions were found mainly in the skull (38% on radiograph and 26% on bone scintigraphy) and proximal femur (29% on radiograph and 26% on bone scintigraphy). Overall there were more lesions found at these sites than any other (Table 2). For solitary lesions, radiograph sensitivity was 95% compared to 88% for bone scintigraphy. All but three of the patients with solitary bone lesions achieved a cure, including one patient with a single rib lesion who was managed by observation alone. The three patients who had chronic disease had multisystem recurrence of LCH. Of the 73 patients, 23 had multisystem involvement and 5 patients with a solitary bone lesion on radiographic survey had LCH involving other organs. Two patients with osseous LCH died. One patient died of systemic amyloidosis 20 yr after diagnosis and the other died of aggressive multisystem LCH 26 yr after diagnosis.

Intraobserver reliability (reproducibility) of bone scintigraphy was 83%–93% for the axial skeleton and 79%–86% for the appendicular skeleton. The regions of highest intraobserver reliability were the skull, facial bones (93%) and the pelvis

TABLE 1
Clinical Details for Patients with Osseous LCH (n = 56)

Mean Age (s.d.)	28 ± 16
Gender (M:F)	30:26
One system only involved	40 (71%)
Co-existing pulmonary LCH	4 (7%)
Co-existing pituitary LCH	7 (12%)
Co-existing skin LCH	13 (23%)
Co-existing lymph node LCH	5 (9%)
Bone pain/tenderness	54 (96%)

(93%). Reporting on the lower extremities yielded the lowest reliability (79%). The 29 bone scans that were reviewed blindly had an interobserver variation of 65%–72% compared to 62%–79% for those studies where clinical information such as the history, physical examination and radiograph findings were made available.

Regional analysis of bone scintigraphy showed poor sensitivity of certain regions including: the pelvis, sacrum, ribs, sternum, clavicles and scapula. The regional group of skull, facial bones and mandible showed higher sensitivity but lower specificity (Table 3). Comparison of bone scintigraphy reporting performed with and without clinical history, findings on physical examination and radiography showed no significant difference ($p > 0.10$, two-tailed) both overall and on regional analysis.

Radiation dosimetry was more favorable for bone scintigraphy. The adult whole-body radiation dose for bone scintigraphy was 2.0 mGy (pediatric: 3.88 mGy) compared to 8.69 mGy (pediatric: 9.99 mGy) for radiographic skeletal survey. Testicular radiation dosimetry favored bone scintigraphy in pediatrics (15.7 mGy versus 18.33 mGy) and adults (1.6 mGy versus 5.19 mGy). Adult ovarian radiation dosimetry also favored bone scintigraphy (2.4 mGy versus 10.78 mGy), but radiographic skeletal survey was more favorable for pediatrics (6.4 mGy versus 10.78 mGy).

DISCUSSION

LCH is a rare disorder that mainly affects children and young adults. Thirty-nine percent of patients were less than 20 yr of age at the time of diagnosis and the mean age of the patients in our sample was 28 yr. This is slightly higher than expected and may be due to an inherent referral bias toward adult patients at our institution (*9*). LCH is a multisystem disease that most commonly affects the bones but also may typically involve the lung, posterior pituitary/hypothalamus, lymph nodes, liver, skin and mucosal membranes (*10*). Seventy-six percent of all patients in this study with the proven histologic diagnosis of LCH had bone involvement. This number concurs with other studies (*11–13*). Higher proportions of osseous LCH have been reported, including a study of 117 patients at the Mayo Clinic between 1907 and 1962, in which there were only five patients without osseous LCH (*14*). In addition, a prospective 29-yr follow-up study of 43 pediatric patients with LCH found osseous lesions had been diagnosed in all 12 surviving patients (*15*). This suggests that the natural history of progressive disease inevitably involves bone.

Solitary Bone Lesion

A solitary osseous lesion was found in 37% of patients with LCH of bone and in 28% of all patients with LCH. The most common sites for the lesion were the skull and proximal femur. Three of the 21 patients who initially presented with solitary osseous LCH had disease recurrence after treatment, and following additional treatment, two achieved prolonged remission. Our data support the findings of other studies that suggest a relatively good prognosis for treated solitary osseous lesions (*16–18*). Multiple osseous lesions found in the remaining 35 patients were predominantly found in the skull, proximal femur and spine. Other published data describing regional analysis of osseous LCH lesions also show similar distribution of lesions (*19*). Studies of smaller patient numbers have shown a more uniform distribution of skeletal lesions (*20*). The absence of spinal lesions in any of the patients with solitary osseous lesions indicates that this area may be a more common site of recurrence than primary disease. Consequently, we recommend that particular attention be paid to the spine when the patient undergoes follow-up surveillance by radiography or bone scintigraphy.

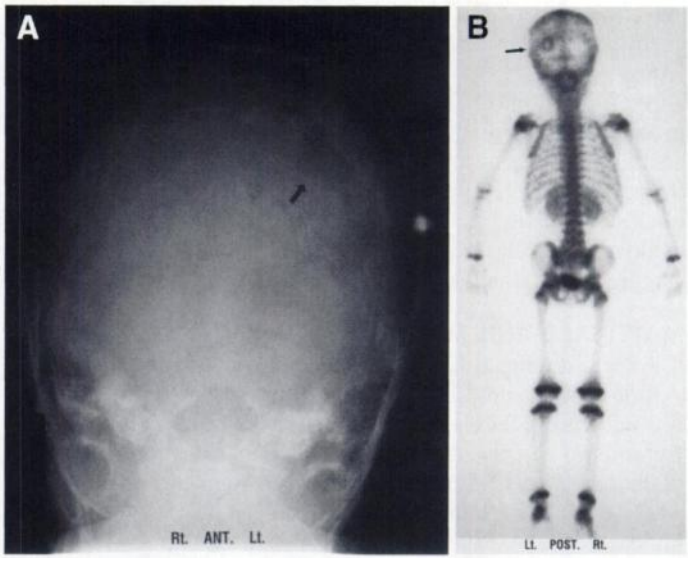

FIGURE 1. Four-year-old boy. (A) Townes radiograph projection of the skull showing a single lucent LCH lesion in the left occipital bone (arrow). (B) Bone scintigraphy (posterior view) shows avid increased radiotracer uptake surrounding a central photopenic area in the left occipital region (arrow). This corresponds to the lesion seen on the radiograph.

Limitations of Bone Scintigraphy

Poor sensitivities for detection of lesions in the pelvis, sacrum, ribs, sternum, clavicle and scapula limit the utility of bone scintigraphy as a diagnostic test. Multifocal osseous LCH lesions have previously been reported to have been missed on bone scintigraphy (*21,22*). Radiographic skeletal survey has been advocated as the best imaging modality to detect multiple

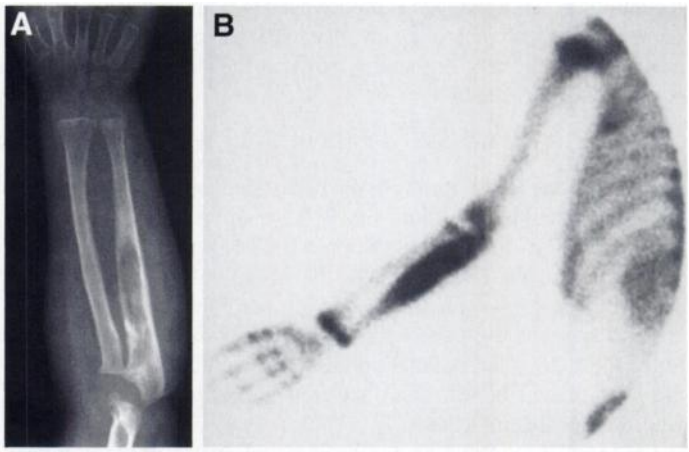

FIGURE 2. Two-year-old boy with biopsy-proven lesion in the left ulna. (A) Radiograph of left forearm shows a lytic destructive lesion in the metaphysis and proximal diaphysis of the ulna. (B) Bone scintigraphy of left upper extremity shows avid radiotracer uptake in the mid and proximal ulna.

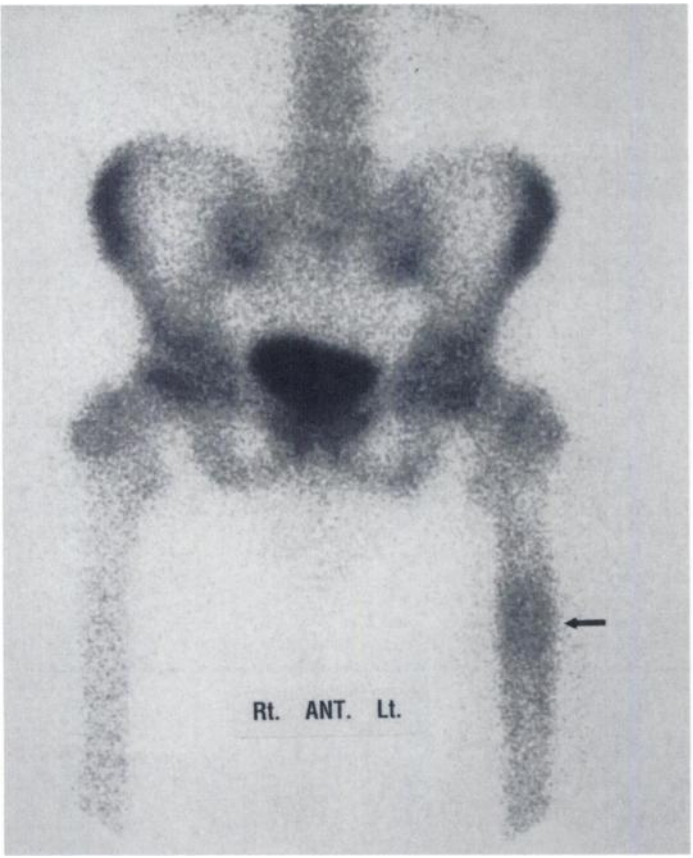

FIGURE 3. Fifteen-year-old boy with biopsy-proven lesion in the left femur. Bone scintigraphy 1 wk after local radiotherapy (1500 cGy in 5 fractions) showing mild diffusely increased radiotracer uptake in the femoral shaft and hyperemic changes secondary to treatment (arrow).

osseous LCH lesions (*20,23*). A study of 16 patients, however, who had no false-negative findings, suggests bone scintigraphy to be a reliable diagnostic tool for the detection of solitary osseous LCH lesions (*24*). For our comparatively older patient population, the scintigraphic sensitivity of solitary lesion detection was 88%. Although this is an acceptable sensitivity, bone scanning adds little diagnostic advantage and patients with solitary bone lesions are best monitored by radiographic survey to exclude local or multiple recurrence.

Role of Bone Scintigraphy

Localized bone pain was found to be a good clinical predictor of bone lesions in patients older than 5 yr. Another study of 36 adult patients with osseous LCH showed local tenderness referable to the bone lesion in 67% of cases (*14*). In most patients, the diagnosis of osseous LCH was made by biopsy after the painful site was depicted as a radiographic lesion. There appears to be no definite role for bone scintigraphy in predicting the best bone biopsy site. The question remains: What is the role of bone scintigraphy in the management of osseous LCH? The answer may be the assessment of response to treatment. Earlier response to therapy of LCH lesions has been shown on bone scintigraphy compared to radiography (*25*). Furthermore, other authors have suggested that recurrences after radiotherapy are more readily detected by bone scintigraphy than radiograph (*26*). On this basis, it could be argued that lesions seen on radiography, but not on bone scintigraphy, are clinically inactive and most likely represent healed or "burned out" lesions. If this is true, bone scintigraphy may be the most sensitive test for the detection of clinically active lesions.

TABLE 2
Distribution of Osseous Lesions on Radiographic Skeletal Survey

	Number		Number
Skull	22	Scapula	1
Facial bones	2	Clavicle	2
Mandible	5	Proximal humerus	10
Cervical spine	1	Distal humerus	2
Thoracic spine	9	Distal upper extremity	2
Lumbosacral spine	6	Proximal femur	17
Pelvis	9	Distal femur	2
Ribs	10	Distal lower extremity	2

TABLE 3
Regional Analysis Showing Relative Diagnostic Accuracy of Bone Scintigraphy

Region (Number of lesions)	Sensitivity (%)	Specificity (%)	+VE predictive (%)	Accuracy (%)
Skull/Facial bones/ Mandible (37)	88	52	41	62
Cervical/Thoracic/ Lumbar spine (23)	50	91	60	83
Pelvis/Sacrum (9)	13	86	25	65
Scapula/Ribs/Sternum/ Clavicle (24)	0	74	0	69
Upper Extremity (13)	50	96	75	86
Lower Extremity (21)	61	62	57	62

Our study suffers from the limitations imposed upon a descriptive study, which includes observer bias. The observers reading both radiographs and bone scans were biased toward the diagnosis of LCH. This also explains why a significant difference was not found between bone scans interpreted with and without clinical history. Unfortunately, a rare disease such as LCH does not easily permit prospective randomized studies which are free of such bias. The use of plain film radiographs as the defacto gold standard for presence of disease is unavoidable but is an additional source of bias.

The relatively unfavorable radiation dosimetry of radiographic skeletal survey to the reproductive organs in adults is of significance for those patients less than 40 yr of age. Radiation protection measures such as accurate collimation of the x-ray beam and the use of lead genital shielding are appropriate. Lead shielding, however, may compromise diagnostic accuracy in the pelvic region. Our results show bone scintigraphy to have relatively poor diagnostic utility in this region and, despite less favorable dosimetry, is not recommended as an alternative to radiography. Although both investigations are comparable in cost, the total cost of whole-body radiographic skeletal survey is slightly less than that of whole-body scintigraphy. MRI has been assessed as an alternative investigation of osseous LCH (*27*). MRI has the advantage of not exposing the patient to ionizing radiation, but this must be balanced against increased cost and prolonged imaging, particularly in children.

CONCLUSION

Whole-body skeletal radiographic survey has greater diagnostic accuracy than whole-body bone scintigraphy for the detection of LCH bone involvement, particularly for the scapula, clavicles, sternum, ribs, pelvis and sacrum, and is the recommended means of staging osseous LCH. Scintigraphy of solitary bone lesions, however, may be useful in monitoring the response to treatment, although further study is required to validate this approach. Our study shows that the most common sites of solitary LCH lesions are the skull and proximal femur and that localizing bone pain is predictive of osseous LCH.

REFERENCES

1. Chu T, D'Angio GJ, Favara B, Ladisch S, Nesbit M, Pritchard J. Histiocytosis syndromes in children. *Lancet* 1987;1:208–209.
2. Resnick D. Lipidoses, Histiocytoses and hyperlipoproteinemias. In: *Diagnosis of bone and joint disorders, 2nd ed.* Philadelphia: W.B. Saunders; 1988:2404–2459.
3. Gilday DL, Ash JM, Reilly BJ. Radionuclide skeletal survey for pediatric neoplasms. *Radiology* 1977;123:399–406.
4. Hanley JA, McNeil BJ. The meaning and use of the area under a receiver operating characteristic (ROC) curve. *Radiology* 1982;143:29–36.
5. Hanley JA, McNeil BJ. A method of comparing the areas under receiver operating characteristic curves derived from the same cases. *Radiology* 1983;148:839–843.
6. The International Commission of Radiological Protection. ICRP Publication 34, Protection of the patient in diagnostic radiology. Oxford, England: Pergamon Press; 1982:53–77.
7. Weber DA, Makler PT, Watson EE, Coffey JL. Radiation absorbed dose from ^{99m}Tc-labeled bone imaging agents. *J Nucl Med* 1989;30:1117–1122.
8. Kereiakis J, Rosenstein M, Bocaraton F. Handbook of radiation doses in nuclear medicine and diagnostic x-ray. Colorado: CRC Press; 1980:165.
9. Berry DH, Becton DL. Natural history of Histiocytosis X. Haem/Oncol Clin N Am 1987;1:23–35.
10. Favara BE, McCarthy RC, Mierau GW. Histiocytosis X. Hum Pathol 1983;14:663–676.
11. Avery ME, McAfee JG, Guild HG. The course and prognosis of reticuloendotheliosis (eosinophilic granuloma, Schuller-Christian disease and Letterer-Siwe disease). A study of forty cases. *Am J Med* 1957;22:636–652.
12. Gianotti F, Caputo R. Histiocytic syndromes: a review. *J Am Acad Dermatol* 1985;13:383–404.
13. Ceci A, De Terlizzi M, Colella R, et al. Langerhans cell histiocytosis in children: results from the Italian co-operative AIEOP-CNR-H.X'83 study. *Med Pediatr Oncol* 1993;21:259–264.
14. Enriquez P, Dahlin DC, Hayles AB, Henderson ED. Histiocytosis X: a clinical study. *Mayo Clin Proc* 1967;42:88–99.
15. Sims DG. Histiocytosis X. Follow-up of 43 cases. *Arch Dis Child* 1977;52:433–440.
16. Cline MJ, Golde DW. A review and re-evaluation of the histiocytic disorders. *Am J Med* 1973;55:49–60.
17. Sartoris DJ, Parker BR. Histiocytosis X: rate and pattern of resolution of osseous lesions. *Radiology* 1984;152:679–684.
18. Martinez-Lage J, Poza M, Cartagena J, Vincente J, Biec F, De Las Heras M. Solitary eosinophilic granuloma of the pediatric skull and spine. *Childs' Nerv Syst* 1991;7:448–451.
19. Schaub T, Ash JM, Gilday DL. Radionuclide imaging in histiocytosis X. *Pediatr Radiol* 1987;17:397–404.
20. Parker BR, Pinckney L, Etcubanas E. Relative efficacy of radiographic and radionuclide bone surveys in the detection of the skeletal lesions of Histiocytosis X. *Radiology* 1980;134:377–380.
21. Antonmattei S, Tetalman MR, Lloyd TV. The multi-scan appearance of eosinophilic granuloma. *Clin Nucl Med* 1979;4:53–55.
22. Kumar R, Balachandran S. Relative roles of radionuclide scanning and radiographic imaging in eosinophilic granuloma. *Clin Nucl Med* 1980;5:538–542.
23. Siddiqui AR, Tashijan JH, Lazarus K, Wellman HN, Baehner RL. Nuclear medicine studies in evaluation of skeletal lesions in children with Histiocytosis X. *Radiology* 1981;140:787–789.
24. Westra SJ, VanWoerden H, Postma A, Elema JD, Piers DA. Radionuclide bone scintigraphy in patients with Histiocytosis X. *Eur J Nucl Med* 1983;8:303–306.
25. Fezoulidis I, Wickenhauser J, Schurawitzki H, Gritzmann N. Histiozytosis X: szintigraphische und rontgenologische Befunde. *Rontgen-Bl* 1987;40:234–239.
26. Crone-Munzebrock W, Brassow F. A comparison of radiographic and bone scan findings in Histiocytosis X. *Skeletal Radiol* 1983;9:170–173.
27. George JC, Buckwalter KA, Cohen MD, Edwards MK, Smith RR. Langerhans cell histiocytosis of bone: MR imaging. *Pediatr Radiol* 1994;24:29–32.

Radionuclide Venography and Its Functional Analysis in Superior Vena Cava Syndrome

Asif Mujtaba Mahmud, Toyoharu Isawa, Takeo Teshima, Tomio Hirano, Yoshiki Anazawa, Makoto Miki and Toshihiro Nukiwa

Department of Respiratory Medicine, Institute of Development, Aging and Cancer (formerly Research Institute for Chest Diseases and Cancer), Tohoku University, Sendai, Japan

In addition to imaging, radionuclide venography maybe used for the functional assessment of superior vena cava (SVC) syndrome by applying the indices of transit time (TT), time of half-peak count (TH) and peak count ratio (PC ratio). **Methods:** Ten healthy subjects (Group N) and 107 patients with SVC syndrome (64 symptomatic and 43 asymptomatic) were studied. Images were visually assessed for collaterals or jugular venous reflux and values of the indices were calculated. **Results:** The 107 patients were subclassified into three groups according to the images obtained. Collateral circulation was seen in 37 patients (Group C). In 20 patients, jugular venous reflux was observed (Group J). Fifty patients who showed neither collaterals nor reflux were included in Group P. In comparison to Group N [3.6 ± 0.56 sec (sem)], TT values were significantly higher ($p < 0.05$) for Group J (7.13 ± 1.16 sec) and Group C (7.00 ± 0.87 sec). Values of TH were significantly prolonged ($p < 0.05$) for Group J (23.6 ± 4.8 sec) and Group C (18.8 ± 2.2 sec) in comparison to Group N (9.2 ± 1.5 sec). PC ratio values were higher in all patient groups in comparison to Group N (3.4 ± 0.57). **Conclusion:** These indices are potentially useful in the initial diagnosis and post-therapeutic evaluation of SVC syndrome. In the absence of other causes, appearance of jugular venous reflux may be considered a sign of SVC syndrome.

Key Words: radionuclide venography; superior vena cava syndrome; jugular venous reflux; functional indices

J Nucl Med 1996; 37:1460–1464

Superior vena cava (SVC) syndrome was first described by William Hunter in 1757 (*1*). Presently, bronchogenic carcinoma is the leading cause and accounts for 67%–82% of all cases of SVC obstruction (*2*). Initially, SVC syndrome was considered to be an oncologic emergency (*3*), but later reports have refuted this notion (*4–6*). Emergency or not, it bears considerable importance for both the clinician and patient.

A careful diagnostic work-up is an essential prerequisite to successful management of this syndrome (*4,6*). Radionuclide venography is a convenient, noninvasive procedure which forms an important component of such a work-up (*2*). In the present study, we intended to establish certain criteria on radionuclide venography to aid in the diagnosis and post-therapeutic evaluation of SVC syndrome and to study hemodynamic characteristics in the central veins, consequent to stenosis and/or obstruction of the SVC.

METHODS

Subjects

Between February 1986 and July 1994, radionuclide venography was performed on 117 subjects. Ten healthy volunteer men (aged 31–57 yr; mean age 43 yr) constituted the control Group N. The remaining 107 were patients with SVC syndrome (97 men, 10 women; age 33–81 yr; mean age 62.6 yr). Selection criteria included presence of clinically obvious SVC syndrome consisting of swelling of the face, neck and/or the upper extremities (symptomatic in 64 patients) or only radiological signs such as mediastinal widening, suprahilar or hilar lesions and tumor location in upper lung zones, rendering them susceptible to SVC syndrome-

Received May 30, 1995; revision accepted Nov. 3, 1995.

For correspondence or reprints contact: Asif Mujtaba Mahmud, Department of Respiratory Medicine, Institute of Development, Aging and Cancer, Tohoku University, 4-1 Seiryoumachi, Aoba-ku, Sendai 980, Japan.